Published in final edited form as:
Science. 2012 August 24; 337(6097): 975–980. doi:10.1126/science.1222278.

PFK1 Glycosylation Is a Key Regulator of Cancer Cell Growth and Central Metabolic Pathways

Wen Yi[1,2], **Peter M. Clark**[1,2], **Daniel E. Mason**[3], **Marie C. Keenan**[4], **Collin Hill**[4], **William A. Goddard III**[5], **Eric C. Peters**[3], **Edward M. Driggers**[4], and **Linda C. Hsieh-Wilson**[1,2,‡]

[1]Division of Chemistry and Chemical Engineering, California Institute of Technology, Pasadena, California 91125, USA

[2]Howard Hughes Medical Institute, California Institute of Technology, Pasadena, California 91125, USA

[3]Genomics Institute of the Novartis Research Foundation, San Diego, California 92121, USA

[4]Agios Pharmaceuticals, 38 Sidney Street, Cambridge, Massachusetts 02139, USA

[5]Materials and Process Simulation Center, California Institute of Technology, Division of Chemistry and Chemical Engineering, 1200 E. California Blvd. Pasadena, CA 91125, USA

Abstract

Cancer cells need to meet the metabolic demands of rapid cell growth within a continually changing microenvironment. Genetic mechanisms for reprogramming cellular metabolism toward proliferative, pro-survival pathways are well-reported. However, post-translational mechanisms, which would enable more rapid, reversible adaptations of cellular metabolism in response to protein signaling or environmental sensing systems, are less well understood. Here we demonstrate that the post-translational modification *O*-linked β-*N*-acetylglucosamine (*O*-GlcNAc) is a key metabolic regulator of glucose metabolism. *O*-GlcNAc is dynamically induced at Ser529 of phosphofructokinase 1 (PFK1) in response to hypoxia. Glycosylation inhibits PFK1 activity and redirects the flux of glucose from glycolysis through the pentose phosphate pathway (PPP), thereby conferring a selective growth advantage to cancer cells. Blocking glycosylation of PFK1 at Ser529 reduced cancer cell proliferation *in vitro* and impaired tumor formation *in vivo*. These studies reveal an unexpected mechanism for the regulation of metabolic enzymes and pathways, and pinpoint a new therapeutic approach for combating cancer.

Rapid physiological response is critical for the growth of tumors, which must satisfy the metabolic demands of increased cell proliferation in the face of a dynamically changing microenvironment. It is now well established that cancer cells undergo significant reprogramming of their cellular metabolism to facilitate the efficient generation of ATP, nucleotide and lipid precursors for macromolecular synthesis, and NADPH to maintain redox homeostasis (1-5). Mutations in tumor suppressors and oncogenic pathways are known to contribute to these altered metabolic phenotypes (1, 6-8), but such changes constitute a slower, more permanent response compared to the rapid, reversible responses needed to adapt to tumor microenvironments *in vivo*. Integration of metabolic flux with rapid-response mechanisms, such as phosphorylation or other post-translational mechanisms, would provide cancer cells with the ability to regulate cellular physiology

‡To whom correspondence should be addressed. lhw@caltech.edu.

Supporting Online Material
www.sciencemag.org/cgi/content/full/

rapidly and reversibly in response to a wide range of signals. However, the post-translational mechanisms that connect signaling pathways to the reprogramming of metabolic flux toward proliferative, pro-survival pathways are poorly understood.

The dynamic post-translational modification *O*-linked β-*N*-acetylglucosamine (*O*-GlcNAc) glycosylation serves as a nutrient sensor to couple metabolic status to the regulation of a wide variety of signaling pathways (9-12). *O*-GlcNAc transferase (OGT) catalyzes the transfer of *N*-acetylglucosamine from uridine diphospho-*N*-acetylglucosamine (UDP-GlcNAc) to serine or threonine residues of many intracellular proteins, including signaling proteins important for insulin resistance (12), oncogenes and tumor suppressors (13,14), and transcriptional co-activators that control gluconeogenesis (15). *O*-GlcNAc levels can be induced within minutes (16), accumulate on the minute-to-hours time scale (17), and are dynamically altered by changes in the cellular concentration of UDP-GlcNAc (9-11). UDP-GlcNAc constitutes the physical integration of several key metabolites, including glucose from glycolysis and carbon supply, glutamine from TCA anapleurosis and nitrogen supply, acetyl-CoA from fatty acid metabolism and NADPH supply, uridine from nucleotide biosynthesis, and ATP from energy charge and oxygen availability (18,19). As such, UDP-GlcNAc may serve as a functional reporter of the status of many important metabolic pathways. Indeed, recent studies have shown that UDP-GlcNAc and the hexosamine biosynthesis pathway couple growth factor-induced glutamine uptake to glucose metabolism via *N*-glycosylation of the IL-3 receptor (18). However, the downstream fates of UDP-GlcNAc, particularly the functional consequences of dynamic *O*-GlcNAc glycosylation in the regulation of cancer cell metabolism, remain unknown.

To gain insight into whether cytoplasmic *O*-GlcNAc glycosylation might directly couple nutrient sensing to cellular metabolism, we modulated *O*-GlcNAc levels and measured the effects on aerobic glycolysis. Global *O*-GlcNAc levels were enhanced by 2-4 fold in the human lung cancer cell line H1299 by overexpression of OGT or by pharmacological inhibition of β-*N*-acetylglucosaminidase (*O*-GlcNAcase or OGA), the glycosidase that removes *O*-GlcNAc (Fig. 1A). Increasing *O*-GlcNAc levels resulted in decreased rates of glucose metabolism (by 23.7±6.7% PUGNAc, 34.6±8.0% OGT overexp), as measured by the conversion of 5-^{3}H-glucose to $^{3}H_2O$, which is catalyzed by enolase in the penultimate step of glycolysis (Fig. 1B). Enhancing *O*-GlcNAc glycosylation also led to reduced lactate production (by 31.3±11.5% PUGNAc, 40.1±8.2% OGT overexp) and lowered cellular ATP levels (by 20.2±6.5% PUGNAc, 22.4±3.7% OGT overexp). Similar effects were observed in other cells, including invasive A549 cancer cells and 293T cells (fig. S1). To confirm that the effects result from the OGT-dependent glycosylation of protein substrates, we produced stable knockdown of OGT in H1299 or 293T cells using shRNA (Fig. 1C and fig. S2). Inhibition of OGA in these OGT-deficient cells had no significant effect on glucose metabolism, lactate production or ATP production (Fig. 1C and fig. S2), suggesting the direct involvement of OGT in the regulation of carbon flow through the glycolytic pathway.

Our proteomics studies had revealed that nearly all of the enzymes in the glycolytic pathway are potential substrates for OGT (20). To determine which enzyme activities are regulated, we modulated *O*-GlcNAc levels in 293T cells as before and measured the activity of each enzyme in the pathway. Increasing *O*-GlcNAc levels significantly decreased (by 15.4±5.8% PUGNAc, 22.6±3.5% OGT-overexp) the activity of phosphofructokinase 1 (PFK1), a major regulatory enzyme long established to control flux through the glycolytic pathway (21) (Fig. 1D). No change in the protein expression levels of PFK1 was observed (fig. S2), indicating that the decrease in activity was not due to reduced PFK1 expression. By contrast, enhancing *O*-GlcNAc levels had only modest effects on other key regulatory points in the pathway, including hexokinase, phosphoglycerate kinase and pyruvate kinase (fig. S3), and no appreciable effect on other glycolytic enzymes.

To establish that PFK1 is directly *O*-GlcNAc glycosylated, we used a chemoenzymatic approach (20) whereby *O*-GlcNAc-modified proteins from 293T cell lysates were selectively labeled with a non-natural azido-sugar using an exogenous glycosyltransferase enzyme, biotinylated using [3+2] azide-alkyne cycloaddition chemistry, and captured with streptavidin-agarose beads (fig. S4). Immunoblotting of the captured proteins with an anti-PFK1 antibody showed a strong signal indicative of *O*-GlcNAc glycosylation of PFK1 (Fig. 1E), which could be further enhanced by overexpression of OGT (fig. S4). We also generated a stable cell line expressing Flag-tagged PFK1 and chemoenzymatically labeled the lysate with a 5-kDa polyethylene glycol (PEG) mass tag to shift the molecular mass of the *O*-GlcNAc-modified species (22). Immunoblotting with an anti-Flag antibody enabled direct visualization of both the non-glycosylated and glycosylated species of Flag-PFK1 (Fig. 1F). Notably, the population of glycosylated PFK1 significantly increased by 15-fold or 6-fold upon OGT overexpression or OGA inhibition, respectively, indicating that glycosylation of PFK1 is reversibly and dynamically regulated by the expression levels or activities of these enzymes. A similar pattern of PFK1 glycosylation was observed in multiple human solid tumor lines (LNCaP, MCF-7, MDA-mb-231, MCF-10-DCIS.com, and MCF-10AT; fig. S5). Moreover, PFK1 glycosylation was induced in a time-dependent manner under hypoxic conditions or when cells were subjected to glucose deprivation (Fig. 1G). Consistent with previous reports that OGT expression and *O*-GlcNAc levels are induced by glucose deprivation and other forms of cell stress (23,24), we observed modest increases in OGT expression levels but found no detectable changes in OGA or PFK1 expression (fig. S6). Thus, PFK1 is *O*-GlcNAc glycosylated in cancer cells and glycosylation is triggered under conditions associated with tumorigenesis and rapid tumor growth.

To identify the glycosylation site(s) on PFK1, FLAG-tagged PFK1 and OGT were transiently co-expressed in 293T cells. After immunoprecipitation and proteolytic digestion of PFK1, *O*-GlcNAc-modified peptides were enriched by WGA lectin affinity chromatography and subjected to electron transfer dissociation mass spectrometry (ETD-MS) analysis. We identified a single site of glycosylation at Ser529, a highly conserved residue important for allosteric regulation of PFK1 by fructose-2,6-bisphosphate (F-2,6-BP) (25) (Fig. 2A and fig. S7). F-2,6-BP is the dominant modulator of PFK1 at the high ATP concentrations (2-5 mM) found in cancer cells (26). Mutation of Ser529 to alanine (S529A) abolished the glycosylation of PFK1 in 293T cells, whereas alanine mutation of the neighboring residue Thr527 had no effect, indicating that Ser529 is the specific, major site of *O*-GlcNAc glycosylation on PFK1 (Fig. 2B).

Although no structure for human PFK1 is available, the enzyme shares 82% sequence identity within the F-2,6-BP binding site with *S. cerevisiae* PFK, which was recently co-crystallized with F-2,6-BP (27), and shares 97% sequence identity with rabbit PFK1, whose apo-structure has been solved (27). To gain insight into the potential effects of glycosylation on F-2,6-BP binding, we used the *S. cerevisiae* structure to generate a homology model of rabbit PFK1 complexed to F-2,6-BP (Fig. 2C). The rmsd between the rabbit and yeast structures was only 1.70 Å, and the 2-phosphate phosphorus of F-2,6-BP in the yeast structure aligned closely with the phosphorus atom of a phosphate ion in the rabbit structure (rmsd 0.25 Å). Moreover, Arg566, Arg655 and His661, which have been shown by mutagenesis to be part of the F-2,6-BP binding site of human PFK1 (25), are found in the predicted rabbit F-2,6-BP binding site. Importantly, we found that Ser529 (Ser530 in rabbit) forms a hydrogen bond with the phosphate ion in the rabbit structure and with the 2-phosphate group of F-2,6-BP in the homology model, suggesting that the addition of a GlcNAc moiety to Ser529 may block the ability of PFK1 to interact with the allosteric activator. As further confirmation, we modeled the *O*-GlcNAc modification on rabbit PFK. The five lowest energy structures showed similar *O*-GlcNAc conformations, with an average

rmsd of 0.59 ± 0.42 Å compared to the lowest energy structure. In all cases, the *O*-GlcNAc moiety occupied the F-2,6-BP-binding pocket and made multiple hydrogen-bonding contacts with the protein (Fig. 2D), suggesting that glycosylation of Ser529 sterically occludes binding of F-2,6-BP. In contrast to F-2,6-BP, the *O*-GlcNAc residue made hydrogen-bonding contacts with only the subunit to which it was covalently bound and formed no hydrogen bonds with the second PFK subunit. Interactions between F-2,6-BP and the two subunits have been proposed to stabilize the PFK dimer in the active conformation (27) and promote the formation of PFK tetramers (25). Thus, our structural models suggest that *O*-GlcNAc glycosylation inhibits PFK1 activity by blocking the binding of F-2,6-BP and possibly perturbing the oligomerization of PFK1 subunits.

We examined the effects of *O*-GlcNAc glycosylation on PFK1 activity by comparing two forms of PFK1 with different levels of glycosylation. Specifically, we tested human Flag-tagged PFK1 expressed in 293T cells in the presence or absence of cellular treatments that enhanced PFK1 glycosylation levels. Increasing *O*-GlcNAc levels on PFK1 resulted in a 35 ± 5% decrease in PFK1 activity (Fig. 2E and fig. S8). By comparison, the same treatments produced no significant change in activity when Ser529 was mutated to alanine. Thus, glycosylation exerts a strong inhibitory effect on PFK1 activity, and this effect is rescued by the S529A mutation. Interestingly, the activity of S529A PFK1 was modestly impaired at lower F-2,6-BP concentrations (fig. S9), consistent with the importance of Ser529 in recognition of the allosteric activator. Glycosylation also inhibited PFK1 activity across a wide ATP concentration range both in the presence and absence of F-2,6-BP (fig. S10). These results demonstrate that *O*-GlcNAc glycosylation of PFK1 at S529 inhibits PFK1 activity, providing a novel mechanism to overcome the allosteric regulation of PFK1 by small molecules.

F-2,6-BP slows the dissociation of high molecular weight complexes of PFK1 and promotes the association of PFK1 into larger aggregates with enhanced catalytic activity (21). To probe whether glycosylation also affects the oligomerization of PFK1, Flag-tagged PFK1 was expressed in 293T cells in the presence or absence of OGT, immunopurified and analyzed by native gel electrophoresis. Upon co-expression with OGT, a significant fraction of PFK1 exhibited greater mobility, indicating formation of a lower molecular weight complex (Fig. 2F). A similar shift in mobility was observed when PFK1 glycosylation levels were increased by treating cells with PUGNAc. Heat denaturation of PFK1 from untreated cells produced a complex of similar mobility, suggesting that this complex represents a lower oligomeric state of PFK1 (fig. S11). To provide further confirmation that glycosylation impairs the association of PFK1 subunits, we examined the ability of Flag-tagged PFK1 to co-immunoprecipitate endogenous PFK1. We found that overexpression of OGT hindered the co-immunoprecipitation of PFK1 subunits, and this effect was blocked by alanine mutation of Ser529 (Fig. 2G). Cumulatively, these results provide strong evidence that *O*-GlcNAc glycosylation not only inhibits the activity of PFK1, but also perturbs the equilibrium between different oligomeric forms to favor a lower oligomeric state. Such a mechanism would enable glycosylated PFK to exert significant effects on the overall PFK1 activity by controlling the balance between high and low activity states.

To create a system to study the functional consequences of Ser529 glycosylation on cellular metabolism, we knocked down endogenous PFK1 and stably expressed Flag-tagged WT or S529A PFK1 in H1299 cells (referred to as WT PFK1 or S529A PFK1 knock-in cells; Fig. 3A). When glycosylation of WT PFK1 was enhanced by overexpression of OGT, the cells exhibited reduced glycolysis and lactate production (by 25.4±5.7% and 37.5±7.3%, respectively; Fig. 3B), consistent with earlier findings (Fig. 1B and fig. S1). Importantly, no change in glycolytic rate or lactate production was observed with the S529A mutant upon

OGT overexpression, indicating that OGT inhibits glycolysis specifically through glycosylation of PFK1 at Ser529.

Suppressing glycolysis via inhibition of PFK1 could lead to the accumulation of glycolytic intermediates and redirect metabolic flux down the oxidative pentose phosphate pathway (PPP). This shift would provide cells with pentose sugars for nucleotides and nucleic acid biosynthesis, as well as reducing equivalents from NADPH to combat oxidative stress (28,29). Increased flux through the oxidative PPP pathway, as measured by the amount of released $^{14}CO_2$ from [1-^{14}C]-glucose, was indeed observed when *O*-GlcNAc levels were enhanced by OGT overexpression in WT PFK1 knock-in cells (Fig. 3C). In contrast, PPP flux remained unaffected by OGT overexpression in S529A PFK1 knock-in cells. The observed increase in PPP activity for S529A PFK1 compared to WT PFK1 knock-in cells was likely due to the modest inhibitory effects of the S529A mutation on PFK1 activity (fig. S9). These results were further confirmed by metabolically labeling the cells with [1,2-^{13}C]-glucose and measuring the relative isotopic enrichment of doubly versus singly [^{13}C]-labeled lactate, pyruvate, and 3-phosphoglycerate by LC-MS analysis, an established method that directly tracks labeled glucose flux simultaneously through glycolysis and the PPP (30). Specifically, a 2.1-fold induction in PPP flux was observed in WT PFK1 knock-in cells upon overexpression of OGT, whereas cells expressing the S529A mutant showed no change (Fig. 3D). Thus, the alteration in pathway flux in a cellular context has been demonstrated using two independent metabolic assays, linking the specific molecular alteration in PFK1 to whole-cell re-regulation of at least two essential pathways, glycolysis and the PPP.

Flux through the PPP generates NADPH, which maintains a pool of reduced glutathione (GSH) and plays an important role in combating reactive oxygen species (ROS)-mediated cell death (31,32). Consistent with increased flux through the PPP, enhancing *O*-GlcNAc levels in WT PFK1 knock-in cells resulted in 1.6-fold and 4-fold inductions in NADPH and GSH levels, respectively (Fig. 3E). Blocking glycosylation of PFK1 at Ser529 fully prevented the increase in NADPH and partially prevented the increase in GSH, demonstrating the importance of *O*-GlcNAc glycosylation at Ser529. Consistent with these observations, untargeted metabolite profiling by high-resolution flow-injection mass spectrometry (33) revealed enhanced steady-state concentrations of GSH, amino acids, and nucleotide precursors in WT PFK1 knock-in cells relative to S529A PFK1 knock-in cells (table S1). Furthermore, we found significant reductions in NADPH and GSH levels in S529A PFK1 knock-in cells compared to WT PFK1 knock-in cells under hypoxic conditions (Fig. 3F), suggesting that S529 has a major role in responding to hypoxia and that blocking PFK1 glycosylation can restore metabolic flux through the glycolysis pathway. To confirm further that glycosylation of PFK1 confers a protective advantage to cancer cells, we measured the sensitivity of H1299 cells to ROS-mediated cell death upon overexpression of OGT. Enhancing *O*-GlcNAc levels prevented the increase in ROS levels induced by diamide (Fig. 3G) and protected the cells from hydrogen peroxide-induced cell death (Fig. 3H). Taken together, the results indicate that increases in PPP flux induced by PFK1 glycosylation have significant consequences for promoting cancer cell survival.

We next investigated the effects of these glycosylation-induced metabolic changes on cell growth. Cells expressing the S529A mutant showed a significantly slower proliferation rate compared to cells expressing WT PFK1 under hypoxic conditions, consistent with decreased flux through the PPP (Fig. 4A). The proliferation rate of WT PFK1-expressing cells was enhanced further upon OGT overexpression, while importantly, that of S529A PFK1-expressing cells was unchanged. To confirm that glycosylation of endogenous PFK1 plays a specific role, we examined the proliferation of OGT overexpression or knockdown cells under hypoxic conditions. OGT overexpression enhanced, while OGT knockdown reduced,

cell proliferation under hypoxic conditions (Fig. 4B). Knocking down PFK1 abolished these effects, indicating that *O*-GlcNAc glycosylation stimulates cell proliferation through a PFK1-dependent mechanism. Thus, glycosylation of PFK1 at Ser529 promotes cell proliferation *in vitro*, and blocking glycosylation reverses the effect.

To determine whether PFK1 glycosylation is important for tumor growth and survival *in vivo*, we injected immunocompromised mice with WT PFK1 or S529A PFK1 knock-in cells in the presence or absence of OGT overexpression (fig. S12) and assayed for tumor formation. Mice injected with S529A PFK1 knock-in cells showed a significant decrease in tumor mass compared to mice injected with WT PFK1 knock-in cells (Fig. 4C). Moreover, overexpression of OGT in WT PFK1 knock-in cells led to enhanced tumor growth, but had no significant effect on S529A PFK1 knock-in cells. Western blot analysis confirmed that the Flag-tagged WT or S529A PFK1 proteins were retained in the tumors and that WT PFK1 was *O*-GlcNAc-modified in the tumors (fig. S12). These results are consistent with the *in vitro* cell proliferation data and demonstrate that glycosylation of PFK1 at Ser529 provides a critical growth advantage to tumors *in vivo*.

Our studies reveal an unexpected mechanism for the regulation of metabolic enzymes – namely, post-translational modification of allosteric sites. Unlike the often-transient interactions of allosteric modulators, the covalent nature of post-translational modifications allows for distinct temporal control, while maintaining the ability to respond reversibly and dynamically to the cell's overall physiological status. Regulation of allosteric sites via post-translational modifications also opens up the opportunity to redirect metabolic flux in response to specific signaling pathways, such as growth factor activation or oxidative stress. Compared to well-established genetic mechanisms for reprogramming metabolic flux (5,34-37), post-translational modifications exert their control on a much faster time-scale, endowing cells with more flexibility to adapt to a constantly changing microenvironment. Through their ability to reversibly modulate a selected subpopulation of the enzyme, post-translational modifications may also allow for more precise control over metabolic enzymes and pathways. Given that many metabolic enzymes have been recently shown to be acetylated, phosphorylated and glycosylated (20,38-39), the post-translational modulation of allosteric sites may represent a general mechanism for integrating the cell's metabolic response with its protein signaling, epigenetic or environmental sensing systems.

Here we demonstrate that *O*-GlcNAc glycosylation directly regulates glycolysis and re-routes metabolic flux through pathways critical for cancer cell proliferation and survival. Although numerous studies have shown that *O*-GlcNAc functions as a metabolic sensor (9-12), our study establishes the first direct role for *O*-GlcNAc as a central regulator of cellular metabolism. These results suggest the existence of dynamic interaction networks, whereby *O*-GlcNAc simultaneously senses and modulates metabolic flow through essential pathways. As UDP-GlcNAc represents a key point of pathway integration and enables the cell to monitor the balance between glucose and glutamine uptake (18,19), *O*-GlcNAc glycosylation of PFK1 may provide a mechanism to link the availability of both carbon and nitrogen sources for the cell to the production of metabolites necessary for sustaining rapid cell growth.

Under conditions of oxidative stress, *O*-GlcNAc glycosylation of PFK1 provides a selective growth advantage to cancer cells by redirecting carbon flow toward the production of precursors necessary for DNA and protein biosynthesis, as well as reducing power in the form of NADPH and GSH to thwart ROS insult. Inhibition of glycolytic enzymes (e.g., triosephosphate isomerase, glyceraldehyde-3-phosphate dehydrogenase and pyruvate kinase M2) via other mechanisms has been shown to lead to re-routing of glucose flux toward anabolic processes (40-42). Our results suggest that inhibition of PFK1, which functions

upstream of these enzymes and is a major classical regulatory point for central carbon flow, exerts profound control over cancer cell metabolism and confers the ability to adapt rapidly to the changing needs and microenvironment of tumor cells. As blocking PFK1 glycosylation enhances its activity and resets the cellular metabolism toward normal cell growth, therapeutics that inhibit PFK1 glycosylation or lead to activation of PFK1 may represent a novel approach to combat cancer.

Supplementary Material

Refer to Web version on PubMed Central for supplementary material.

Acknowledgments

We thank P. Qasba (National Cancer Institute) for the Y289L GalT construct, S.-H. Yu for synthesizing the UDP-ketogalactose substrate, and R. Abrol for assistance with the computational modeling. We would like to acknowledge L. Cantley for reading the manuscript and useful discussions. This work was supported by the National Institutes of Health (R01 GM084724 to L.C.H-W), the Department of Defense Breast Cancer Research Program (W81XWH-10-1-0988 to W.Y), and a Tobacco-Related Disease Research Program Postdoctoral Fellowship (19FT-0078 to W.Y).

References

1. DeBerardinis RJ, Lum JJ, Hatzivassiliou G, Thompson CB. The biology of cancer: metabolic reprogramming fuels cell growth and proliferation. Cell Metab. 2008; 7:11–20. [PubMed: 18177721]
2. Vander Heiden MG, Cantley LC, Thompson CB. Understanding the Warburg effect: The metabolic requirements of cell proliferation. Science. 2009; 324:1029. [PubMed: 19460998]
3. Hsu PP, Sabatini DM. Cancer cell metabolism: Warburg and beyond. Cell. 2008; 134:703. [PubMed: 18775299]
4. Cairns RA, Harris IS, Mak TW. Regulation of cancer cell metabolism. Nat Rev Cancer. 2011; 11:85. [PubMed: 21258394]
5. Christofk HR, et al. The M2 splice isoform of pyruvate kinase is important for cancer metabolism and tumor growth. Nature. 2008; 452:230. [PubMed: 18337823]
6. Dang CV, Kim J, Gao P, Yustein J. The interplay between Myc and HIF in cancer. Nat. Rev. Cancer. 2008; 8:51. [PubMed: 18046334]
7. Levine AJ, Puzio-Kuter AM. The control of the metabolic switch in cancers by oncogenes and tumor suppressor genes. Science. 2010; 330:1340. [PubMed: 21127244]
8. Shaw RJ, Cantley LC. Ras, PI(3)K and mTOR signalling controls tumor cell growth. Nature. 2006; 441:424. [PubMed: 16724053]
9. Rexach JE, Clark PM, Hsieh-Wilson LC. Chemical approaches to understanding O-GlcNAc glycosylation in the brain. Nat. Chem. Biol. 2008; 4:97. [PubMed: 18202679]
10. Hart GW, Housley MP, Slawson C. Cycling of O-linked β-N-acetylglucosamine on nucleocytoplasmic proteins. Nature. 2007; 446:1017. [PubMed: 17460662]
11. Love DC, Hanover JA. The hexosamine signalling pathway: Deciphering the “O-GlcNAc code”. Sci STKE. 2005; 2005:re13. [PubMed: 16317114]
12. Yang X, et al. Phosphoinositide signalling links O-GlcNAc transferase to insulin resistance. Nature. 2008; 451:964. [PubMed: 18288188]
13. Yang WH, et al. Modification of p53 with O-linked N-acetylglucosamine regulates p53 activity and stability. Nat. Cell Biol. 2006; 8:1074. [PubMed: 16964247]
14. Chou TY, Hart GW, Dang CV. c-Myc is glycosylated at threonine 58, a known phosphorylation site and a mutational hot spot in lymphomas. J. Biol. Chem. 1995; 270:18961. [PubMed: 7642555]
15. Dentin R, et al. Hepatic glucose sensing via the CREB coactivator CRTC2. Science. 2008; 319:1402. [PubMed: 18323454]

16. Kneass ZT, Marchase RB. Neutrophils exhibit rapid agonist-induced increases in protein-associated O-GlcNAc. J. Biol. Chem. 2004; 279:45759. [PubMed: 15322139]
17. Rexach JE, et al. In Press. Dynamic O-GlcNAc Glycosylation regulates CREB-mediated gene expression and memory formation. Nat. Chem. Biol. 2011
18. Wellen KE, et al. The hexosamine biosynthetic pathway couples growth factor-induced glutamine uptake to glucose metabolism. Genes Dev. 2010; 24:2784. [PubMed: 21106670]
19. Moseley HN, et al. A novel deconvolution method for modeling UDP-N-acetyl-D-glucosamine biosynthetic pathways based on ^{13}C mass isotopologue profiles under non-steady-state conditions. BMC Biol. 2011; 9:37. [PubMed: 21627825]
20. Clark PM, et al. Direct in-gel fluorescence detection and cellular imaging of O-GlcNAc-modified proteins. J Am Chem Soc. 2008; 130:11576. [PubMed: 18683930]
21. Sola-Penna M, et al. Regulation of mammalian muscle type 6-phosphofructo-1-kinase and its implication for the control of the metabolism. IUBMB Life. 2010; 62:791. [PubMed: 21117169]
22. Rexach JE, et al. Quantification of O-glycosylation stoichiometry and dynamics using resolvable mass tags. Nat Chem Biol. 2010; 6:645. [PubMed: 20657584]
23. Zachara NE, et al. Dynamic O-GlcNAc modification of nucleocytoplasmic proteins in response to stress. J. Biol. Chem. 2004; 279:30133. [PubMed: 15138254]
24. Taylor RP, et al. Glucose deprivation stimulates O-GlcNAc modification of proteins through up-regulation of O-linked N-acetylglucosaminyltransferase. J. Biol. Chem. 2008; 283:6050. [PubMed: 18174169]
25. Ferreras C, et al. Subunit interactions and composition of the fructose-6-phosphate catalytic site and the fructose 2,6-bisphosphate allosteric site of mammalian phosphofructokinase. J. Biol. Chem. 2009; 284:9124. [PubMed: 19218242]
26. Lu X, et al. Cellular ATP depletion by LY309887 as a predictor of growth inhibition in human tumor cell lines. Clin. Cancer Res. 2000; 6:271. [PubMed: 10656458]
27. Banaszak K, et al. The crystal structures of eukaryotic phosphofructokinases from Baker's yeast and rabbit skeletal muscle. J. Mol. Biol. 2011; 407:284. [PubMed: 21241708]
28. Tong X, Zhao F, Thompson CB. The molecular determinants of de novo nucleotide biosynthesis in cancer cells. Curr. Opin. Genet. Dev. 2009; 19:32. [PubMed: 19201187]
29. Tennant DA, Duran RV, Gottlieb E. Targeting metablic transformation for cancer therapy. Nat. Rev. Cancer. 2010; 10:267. [PubMed: 20300106]
30. Munger J, et al. Systems-level metabolic flux profiling identifies fatty acid synthesis as a target for antiviral therapy. Nat. Biotechnol. 2008; 26:1179. [PubMed: 18820684]
31. Pandolfi PP, et al. Targeted disruption of the housekeeping gen encoding glucose 6-phosphate dehydrogenase (G6PD): G6PD is dispensable for pentose synthesis but essential for defense against oxidative stress. EMBO J. 1995; 14:5209. [PubMed: 7489710]
32. Bensaad K, et al. TIGAR, a p53-inducible regulator of glycolysis and apoptosis. Cell. 2006; 126:107. [PubMed: 16839880]
33. Fuhrer T, Heer D, Begemann B, Zamboni N. High-throughput, accurate mass metabolome profiling of cellular extracts by Flow-Injection-Time-of-Flight Mass Spectrometry. Anal. Chem. 2011; 83:7074. [PubMed: 21830798]
34. Dang L, et al. Cancer-associated IDH1 mutations produce 2-hydroxyglutarate. Nature. 2009; 462:739. [PubMed: 19935646]
35. Possemato R, et al. Functional genomics reveal that the serine synthesis pathway is essential in breast cancer. Nature. 2011; 476:346. [PubMed: 21760589]
36. Gao P, et al. c-Myc suppression of miR-23a/b enhances mitochondrial glutaminase expression and glutamine metabolism. Nature. 2009; 458:762. [PubMed: 19219026]
37. Shakya A, et al. Oct1 loss of function induces a coordinate metabolic shift that opposes tumorigenicity. Nat. Cell Biol. 2009; 11:320. [PubMed: 19219035]
38. Zhao S, et al. Regulation of cellular metabolism by protein lysine acetylation. Science. 2010; 327:1000. [PubMed: 20167786]
39. Hitosugi T, et al. Tyrosine phosphorylation inhibits PKM2 to promote the Warburg effect and tumor growth. Sci. Signal. 2009; 2:ra73. [PubMed: 19920251]

40. Christofk HR, et al. Pyruvate kinase M2 is a phosphotyrosine-binding protein. Nature. 2008; 452:181. [PubMed: 18337815]
41. Ralser M, et al. Dynamic rerouting of the carbohydrate flux is key to counteracting oxidative stress. J. Biol. 2007; 6:10. [PubMed: 18154684]
42. Ralser M, et al. Triose phosphate isomerase deficiency is caused by altered dimerization-not catalytic inactivity-of the mutant enzymes. PLoS ONE. 2006; 1:e30. [PubMed: 17183658]

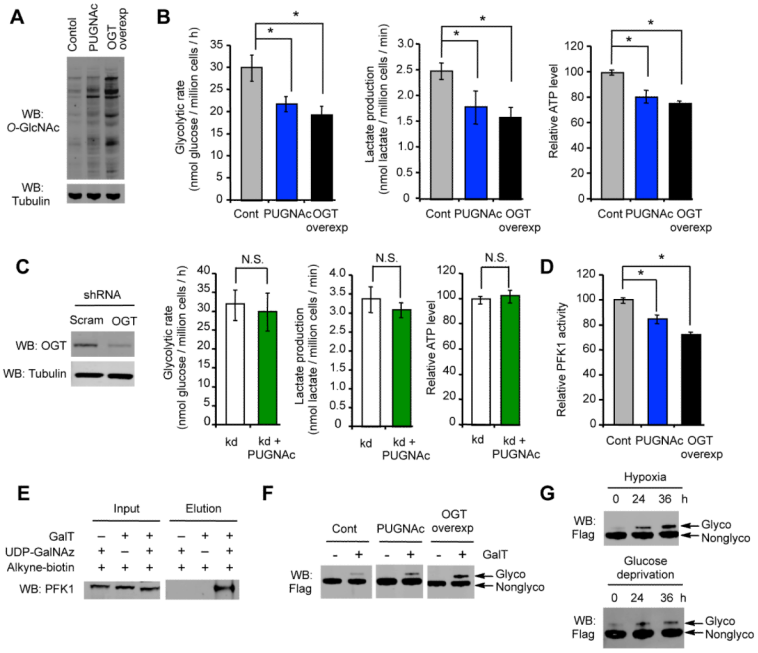

Fig. 1. Modulation of *O*-GlcNAc levels affects cellular metabolism and glycosylation of PFK1

(**A**) *O*-GlcNAc glycosylation levels as determined by immunoblotting with an anti-*O*-GlcNAc antibody after treatment of H1299 cells with the OGA inhibitor *O*-(2-acetamido-2-deoxy-D-glucopyranosylidene)amino-*N*-phenylcarbamate (PUGNAc) or OGT overexpression. Tubulin levels demonstrate equal protein loading. (**B**) Glycolytic rate, lactate production and relative ATP levels in untreated H1299 cells (Cont), PUGNAc-treated H1299 cells and H1299 cells overexpressing OGT ($n = 5$). (**C**) OGT levels in H1299 cells transfected with scramble or OGT shRNA. Tubulin levels demonstrate equal protein loading. Glycolytic rate, lactate production and relative ATP levels of H1299 cells transfected with OGT shRNA (kd) upon treatment with or without PUGNAc ($n = 4$; N.S., Not Significant). (**D**) PFK1 activity in untreated 293T cells (Cont), PUGNAc-treated 293T cells and 293T cells overexpressing OGT ($n = 5$). (**E**) Detection of PFK1 glycosylation by Western blotting after chemoenzymatic labeling of *O*-GlcNAc residues with UDP-GalNAz and the enzyme GalT, followed by reaction with an alkyne-biotin derivative, streptavidin pull-down and elution of the biotinylated proteins. GalT and UDP-GalNAz were removed as a control to confirm the specific labeling of *O*-GlcNAc. (**F**) Detection of glycosylated PFK1 levels in 293T cells stably expressing Flag-tagged PFK1 by chemoenzymatic labeling with a 5-kDa mass tag and immunoblotting with an anti-Flag antibody. Cells were untreated (Cont), treated with PUGNAc or transfected to overexpress OGT. (**G**) PFK1 glycosylation levels under hypoxic conditions or glucose deprivation. Levels were detected in H1299 cells stably expressing Flag-tagged PFK1 by chemoenzymatic labeling with a 5-kDa mass tag as described above. Error bars denote s.e.m. Statistical analysis was performed by Student's *t*-test (* $P < 0.05$) for all figures.

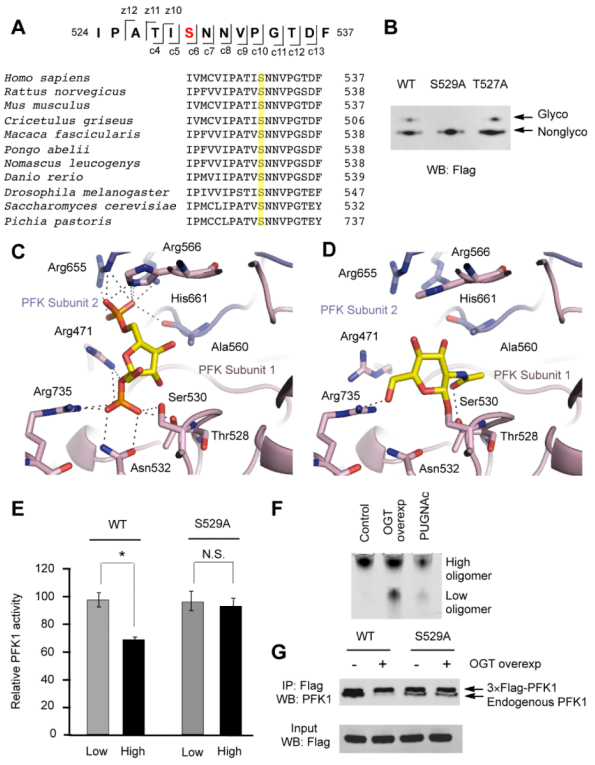

Fig. 2. Glycosylation within the F-2,6-BP binding site of PFK1 inhibits its activity and oligomerization

(**A**) Peptide sequence and glycosylation site (red) identified by ETD-MS (*top*). Sequence alignment of the residues surrounding Ser529 of PFK1 across different species (*bottom*). (**B**) Glycosylation levels of Flag-tagged WT PFK1 and PFK1 mutants as determined by chemoenzymatic labeling with a 5-kDa PEG mass tag followed by immunoblotting with an anti-Flag antibody. (**C**) Homology model of F-2,6-BP (yellow) bound to rabbit PFK1. (**D**) Computational model of rabbit PFK1 *O*-GlcNAc glycosylated (yellow) at Ser530, the residue equivalent to Ser529 in human PFK1. (**E**) Relative activities of WT and S529A PFK1 purified from transfected 293T cells with (High) and without (Low) treatments to enhance PFK1 glycosylation levels. Activities were measured in the presence of 100 μM F-2,6-BP and 3 mM ATP and were normalized with respect to the activity of WT PFK1 without treatment ($n = 3$). (**F**) Oligomerization state of Flag-tagged PFK1 purified from untreated 293T cells (Cont), and 293T cells following treatment with PUGNAc or OGT overexpression. (**G**) Co-immunoprecipitation of endogenous PFK1 with Flag-tagged WT or S529A PFK1 following OGT overexpression. Error bars denote s.e.m. Statistical analysis was performed by Student's *t*-test (* $P < 0.05$) for all figures.

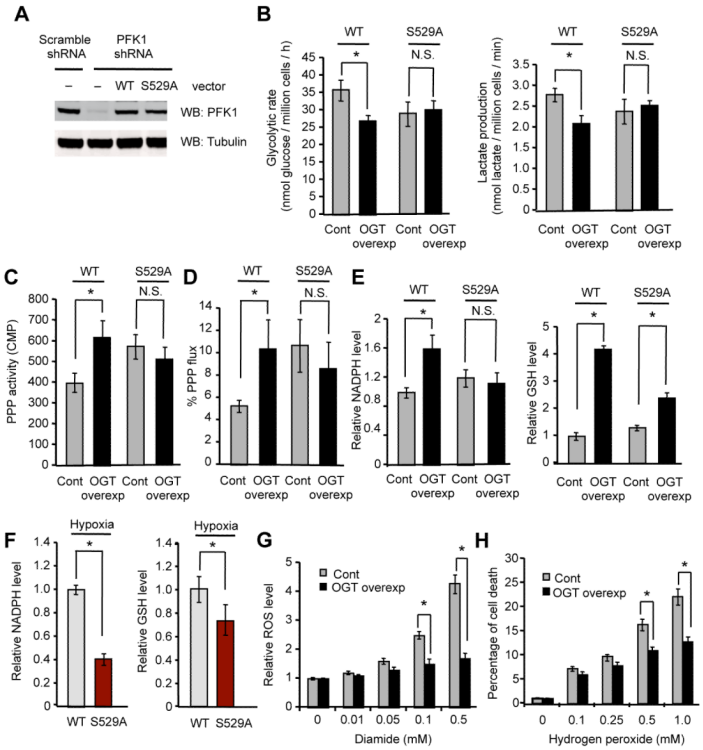

Fig. 3. PFK1 glycosylation at Ser529 regulates glycolysis, increases PPP flux and protects cells from ROS-mediated cell death

(**A**) Immunoblotting of H1299 cells stably expressing shRNA constructs and rescue constructs. Cells were infected with lentivirus containing shRNA-resistant Flag-WT or S529A PFK1 constructs where indicated, selected for 2 weeks and then infected with lentivirus containing scramble or PFK1 shRNA constructs to knockdown endogenous PFK1 expression. Tubulin levels demonstrate equal protein loading. Flag-PFK1 levels were comparable to endogenous PFK1 levels. (**B**) Glycolytic rate and lactate production of H1299 knock-in cells expressing WT or S529A PFK1 in the absence (Cont) or presence of OGT overexpression ($n = 4$). (**C**) PPP activity in WT or S529A PFK1 knock-in cells in the absence (Cont) or presence of OGT overexpression. PPP activity was calculated as the difference between the rate of [1-^{14}C]-glucose and [6-^{14}C]-glucose oxidation to [^{14}C]-CO_2 ($n = 3$). (**D**) Percentage of central carbon flux from glucose to lactate flowing through the PPP in WT or S529A PFK1 knock-in cells in the absence (Cont) or presence of OGT overexpression. Flux was determined from the relative enrichment of doubly vs. singly [^{13}C]-labeled lactate, pyruvate, and 3-phosphoglycerate, as measured using negative mode triple-quadrupole LC-MS of extracts from cells fed with [1,2-^{13}C]-glucose. (**E**) NADPH and GSH levels in WT or S529A PFK1 knock-in cells in the absence (Cont) or presence of OGT overexpression. NADPH levels were measured using a colorimetric assay (BioVison). GSH levels were measured by fluorimetric detection of the binding of the thiol probe monochlorobimane to the free GSH. Levels are shown relative to WT PFK1 Cont ($n = 4$). (**F**) NADPH and GSH levels in WT or S529A PFK1 knock-in cells under hypoxic conditions ($n = 3$). (**G**) Cellular ROS levels induced by varying concentrations of diamide in untreated H1299 cells (Cont) and H1299 cells overexpressing OGT, as measured by oxidation of the dye CM-H_2DCFDA. (**H**) Percentage of cell death induced by varying concentrations of hydrogen peroxide in untreated H1299 cells (Cont) and H1299 cells overexpressing OGT, as measured by media lactate dehydrogenase levels ($n = 4$). Error bars

denote s.e.m. Statistical analysis was performed by Student's *t*-test (* $P < 0.05$) for all figures.

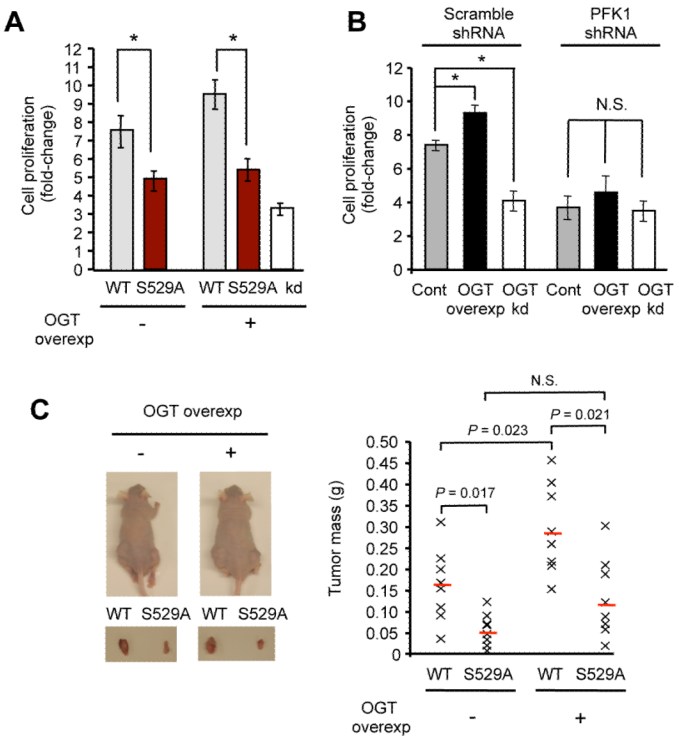

Fig. 4. Blocking PFK1 glycosylation slows cell proliferation and reduces the tumorigenicity of lung cancer cells

(**A**) Cell proliferation rates under hypoxic conditions of WT and S529A PFK1 H1299 knock-in cells with and without OGT overexpression ($n = 3$; * $P < 0.05$, N.S., Not Significant). (**B**) Cell proliferation rates under hypoxic conditions of H1299 cells infected with lentiviruses containing scramble or PFK1 shRNA constructs following no treatment (Cont), OGT knockdown or OGT overexpression ($n = 3$; * $P < 0.05$). (**C**) Tumor formation in nude mice injected with WT or S529A PFK1 H1299 knock-in cells with and without OGT overexpression. Dissected tumors after 7-weeks growth in mice injected with WT cells on the left flank and S529A cells on the right flank (left). Masses of the dissected tumors (right). Each x represents the tumor mass from one mouse; the blue line indicates the mean tumor mass. Error bars denote s.e.m. Statistical analysis was performed by Student's *t*-test for all figures.